Persistence of ctDNA in Patients with Breast Cancer During Neoadjuvant Treatment Is a Significant Predictor of Poor Tumor Response

Qing Zhou[1,2], Simon P. Gampenrieder[3,4,5], Sophie Frantal[6], Gabriel Rinnerthaler[3,4,5], Christian F. Singer[7], Daniel Egle[8], Georg Pfeiler[7], Rupert Bartsch[9], Viktor Wette[10], Angelika Pichler[11], Edgar Petru[12], Peter C. Dubsky[13,14], Zsuzsanna Bago-Horvath[13], Christian Fesl[4], Margaretha Rudas[15], Anders Ståhlberg[16,17,18], Ricarda Graf[1], Sabrina Weber[1], Nadia Dandachi[19], Martin Filipits[20], Michael Gnant[21], Marija Balic[19], and Ellen Heitzer[1,2]; on behalf of the ABCSG

ABSTRACT

Purpose: Accurate response assessment during neoadjuvant systemic treatment (NST) poses a clinical challenge. Therefore, a minimally invasive assessment of tumor response based on cell-free circulating tumor DNA (ctDNA) may be beneficial to guide treatment decisions.

Experimental Design: We profiled 93 genes in tissue from 193 patients with early breast cancer. Patient-specific assays were designed for 145 patients to track ctDNA during NST in plasma. ctDNA presence and levels were correlated with complete pathological response (pCR) and residual cancer burden (RCB) as well as clinicopathologic characteristics of the tumor to identify potential proxies for ctDNA release.

Results: At baseline, ctDNA could be detected in 63/145 (43.4%) patients and persisted in 25/63 (39.7%) patients at mid-therapy (MT) and 15/63 (23.8%) patients at the end of treatment. ctDNA detection at MT was significantly associated with higher RCB (OR = 0.062; 95% CI, 0.01–0.48; $P = 0.0077$). Of 31 patients with detectable ctDNA at MT, 30 patients (96.8%) were nonresponders (RCB II, $n = 8$; RCB III, $n = 22$) and only one patient responded to the treatment (RCB I). Considering all 145 patients with baseline (BL) plasma, none of the patients with RCB 0 and only 6.7% of patients with RCB I had ctDNA detectable at MT, whereas 30.6% and 29.6% of patients with RCB II/III, respectively, had a positive ctDNA result.

Conclusions: Overall, our results demonstrate that the detection and persistence of ctDNA at MT may have the potential to negatively predict response to neoadjuvant treatment and identify patients who will not achieve pCR or be classified with RCB II/III.

Introduction

Neoadjuvant systemic therapy (NST) is a well-established treatment for patients with early breast cancer (EBC) with high-risk features such as advanced clinical stage, estrogen receptor negativity or HER2 positivity. NST not only reduces tumor burden, thereby allowing a greater number of patients to undergo breast conservation therapy, but also reduces the risk for tumor recurrence in the same way as adjuvant therapy does (1). A major challenge in the neoadjuvant setting is, however, the prediction of response to NST before surgery, which could serve as the basis for escalating treatment in nonresponders and de-escalating treatment in responders, respectively (2–5). To date, neither imaging methods like ultrasound (6) or MRI (7) nor image-guided breast biopsies before surgery (8–10) have been able to

[1]Institute of Human Genetics, Diagnostic & Research Center for Molecular BioMedicine, Medical University of Graz, Graz, Austria. [2]Christian Doppler Laboratory for Liquid Biopsies for Early Detection of Cancer, Medical University of Graz, Graz, Austria. [3]IIIrd Medical Department with Hematology and Medical Oncology, Hemostaseology, Rheumatology and Infectious Diseases, Oncologic Center, Paracelsus Medical University Salzburg, Salzburg, Austria. [4]Salzburg Cancer Research Institute with Laboratory of Immunological and Molecular Cancer Research (LIMCR) and Center for Clinical Cancer and Immunology Trials (CCCIT), Salzburg, Austria. [5]Cancer Cluster Salzburg, Salzburg, Austria. [6]Department of Statistics, Austrian Breast and Colorectal Cancer Study Group, Vienna, Austria. [7]Department of Gynecology and Gynecological Oncology, Comprehensive Cancer Center, Medical University of Vienna, Vienna, Austria. [8]Department of Obstetrics and Gynecology, Medical University Innsbruck, Innsbruck, Austria. [9]Division of Oncology, Department of Medicine I, Medical University of Vienna, Vienna, Austria. [10]Breast Center, Brustzentrum Kaernten, St. Veit, Austria. [11]Department of Hemato-Oncology, LKH Hochsteiermark-Leoben, Leoben, Austria. [12]Department of Gynaecology and Obstetrics, Medical University Graz, Graz, Austria. [13]Department of Surgery and Comprehensive Cancer Center, Medical University of Vienna, Vienna, Austria. [14]Breast Center St. Anna, Lucerne, Switzerland. [15]Department of Pathology, Medical University of Vienna, Vienna, Austria. [16]Department of Laboratory Medicine, Sahlgrenska Center for Cancer Research, Institute of Biomedicine, Sahlgrenska Academy at University of Gothenburg, Gothenburg, Sweden. [17]Wallenberg Centre for Molecular and Translational Medicine, University of Gothenburg, Gothenburg, Sweden. [18]Region Västra Götaland, Sahlgrenska University Hospital, Department of Clinical Genetics and Genomics, Gothenburg, Sweden. [19]Division of Oncology, Department of Internal Medicine, Medical University Graz, Graz, Austria. [20]Department of Medicine I, Comprehensive Cancer Center, Institute of Cancer Research, Medical University of Vienna, Vienna, Austria. [21]Comprehensive Cancer Center, Medical University of Vienna, Vienna, Austria.

Note: Supplementary data for this article are available at Clinical Cancer Research Online (http://clincancerres.aacrjournals.org/).

M. Balic and E. Heitzer contributed equally to this article.

Corresponding Authors: Ellen Heitzer, D&R Institute of Human Genetics, Medical University of Graz, Neue Stiftingtalstrasse 6, Graz, 8010, Austria. E-mail: ellen.heitzer@medunigraz.at; and Marija Balic, Department of Internal Medicine, Division of Oncology, Medical University Graz, Auenbruggerplatz 15, 8010 Graz, Austria. E-mail: marija.balic@medunigraz.at

Clin Cancer Res 2022;28:697–707

doi: 10.1158/1078-0432.CCR-21-3231

Translational Relevance

In this translational study, we tested the use of ctDNA to predict response to neoadjuvant systemic therapy (NST) in patients with early breast cancer ($n = 145$) recruited to a prospective, randomized, neoadjuvant phase II study. By the use of patient-specific high-resolution assays, we demonstrate that the detection and persistence of ctDNA in the middle of NST may have the potential to negatively predict response to treatment and identify patients who will not achieve pCR or be classified with RCB II/III. A noninvasive identification of RCB may have the potential to aid clinical decision-making with respect to treatment escalation in non-responders, who are known to benefit from additional adjuvant therapy, or de-escalation by identifying patients who might not derive benefit from breast surgery after NST.

adequately predict pathologic complete response (pCR). Therefore, a minimally-invasive assessment or prediction of tumor response earlier during NST may be highly beneficial for guiding treatment decisions.

Liquid biopsies, that is, the analysis of tumor components floating in body fluids such as blood, have shown promising clinical utility in many solid tumors (11–14). Recent studies have indicated the utility of using circulating tumor DNA (ctDNA) in EBC patients. For example, Garcia-Murilla and colleagues demonstrated that the detection of ctDNA during follow-up is associated with a high risk of future relapse of EBC (15). Other groups reported that during NST, a quick decline of ctDNA levels is associated with undetectable minimal residual disease or pCR (16, 17). The presence of ctDNA towards the end of the treatment (EOT) has reflected residual disease (18). Moreover, one recent study demonstrated that the detection of ctDNA before neoadjuvant anti-HER2 therapies is associated with decreased pCR rates (19). Magbanua and colleagues reported that persistence of ctDNA during NST is a significant predictor of poor response and metastatic recurrence (20).

We tested the use of ctDNA to predict response to NST in patients with EBC recruited to a prospective, randomized, neoadjuvant phase II study (ABCSG-34). In this study, the efficacy and safety of tecemotide, a liposome-based, antigen-specific cancer immunotherapy designed to elicit a cellular immune response against MUC1, when added to neoadjuvant standard-of-care (SoC) treatment was investigated (21, 22). To this end, we profiled primary tissue using a 93-gene panel and designed patient-specific assays for high-resolution tracking of ctDNA in plasma prior to, at the middle of, and at the end of treatment, respectively. In contrast to previous studies, we assessed not only pCR rates but also the residual cancer burden (RCB) as an endpoint, which has been demonstrated as a more accurate long-term predictor of disease recurrence and survival across all breast cancer subtypes (23, 24). Furthermore, we associated the presence and levels of ctDNA with clinicopathologic characteristics of the tumor to identify proxies for ctDNA release. As a secondary aim, tumor driver alterations obtained from mutation analysis and genome-wide somatic copy-number alterations (SCNA) detected from shallow whole-genome sequencing (sWGS) were associated with response and clinicopathologic features of the tumors.

Materials and Methods

The clinical trial was conducted according to the principles of the Declaration of Helsinki and the ICH Guidelines (EudraCT#: 2011-004822-85) and was approved by the appropriate Ethics Committees of each of the participating centers before study initiation. All patients provided written informed consent. The translational part reported in this manuscript was approved by the Ethics Committee of the Medical University of Graz (27-500 ex 14/15).

Patient cohort

This study included 193 patients with hormone receptor-positive (HR+; estrogen/progesterone receptor + or higher) HER2-negative and triple-negative (TNBC: HR−, and HER2−) tumors from the prospective, randomized, multicenter phase II ABCSG-34 trial (21). If detailed subtype information was lacking, the definition for HR high and low tumors was used and all such tumors were considered as HR+. Other lacking subtype information was kept as missing and such tumors were excluded from the subsequent analysis. For patients who experienced bilateral cancer ($n = 2$), only information from the worse side was used [based on the baseline prognostic factors nodal status, tumor size, tumor grade, HR status, HER2 status, and Ki-67 (in this order)]. On the basis of hormone receptor (HR) expression, menopausal status, histopathologic grade, and Ki-67, patients were randomized 1:1 to receive chemotherapy (NCT) or endocrine therapy alone (NET) or in combination with the therapeutic cancer vaccine tecemotide (formerly known as Stimuvax or L-BLP25). Although the use of tecemotide was safe, it neither improved pCR nor RCB rates (21), which is why the administration of tecemotide was neglected for this study. Patients with NCT received conventional (anthracycline/cyclophosphamide followed by taxane) or reverse sequence chemotherapy, again without impact on response (22).

Blood and tumor tissue samples were obtained prior to treatment initiation (baseline, BL), after four cycles of chemotherapy (conventional and reverse sequence arms) or after 12 weeks of aromatase inhibitor treatment (endocrine arm) (mid-therapy, MT) and at surgery (EOT; **Fig. 1A**). Although tissue was analyzed only at BL and was available for all patients, blood was available for 145 patients, with 108 patients having blood drawn at all three time points (**Fig. 1B**). From 92 of 145 patients with available plasma, EndoPredict data were available from a previous study (25).

Assessment of clinicopathologic features and response

Immunohistochemical Ki-67 expression and tumor grade according to Elston and Ellis (Ventana Benchmark Ultra) were centrally determined by an experienced breast cancer pathologist. The logarithm of Ki-67 values was used for all analyses to approximate a normal distribution. For classification into high and low, two different cut-offs (14% and 20%) were used. Stromal and intratumoral tumor infiltrating lymphocytes (TILs) were also centrally determined and analyzed as previously described (26, 27). For classification into high and low a 19% threshold was used. A subset of diagnostic cores was tested using EndoPredict (Myriad International GmbH) at the University of Vienna according to manufacturer's instructions as previously described (25, 28–30). Tumor response was assessed as residual breast cancer burden (RCB) based on the index developed from Symmans and colleagues (31) and pathological complete response (pCR), respectively. RCB was assessed and confirmed by central pathological review and patients were stratified into responders (RCB 0/I, RCB index ≤1.36) and nonresponders (RCB II/III, RCB index >1.36). Pathologic complete response (pCR) was defined as ypT0/is ypN0 in the surgical specimen.

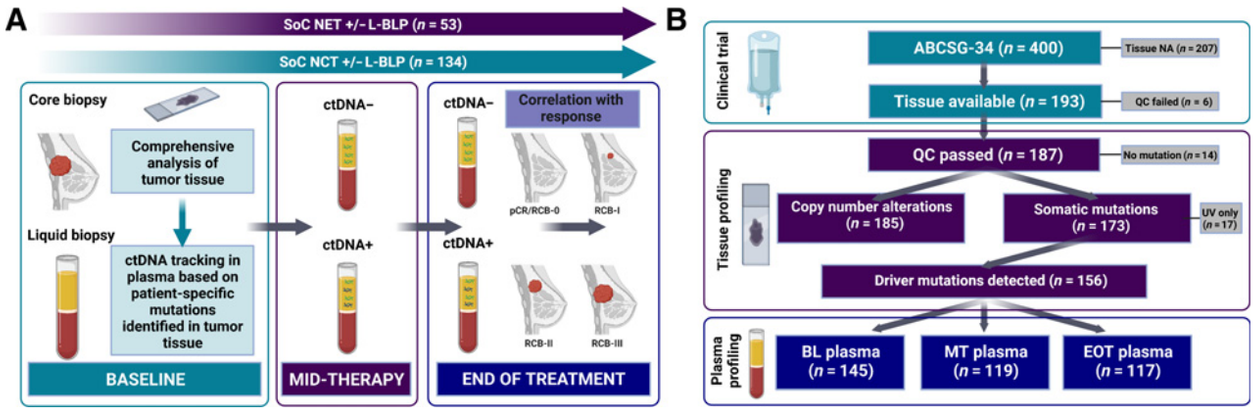

Figure 1.

Study design and flow chart and molecular profiling results. **A,** Shown is an overview of the study design. Patients with early breast cancer were treated with standard of care (SoC) NCT or NET. After mutation analysis of the primary tumors using a 93-gene panel, patient-specific high-resolution assays were designed to track ctDNA during treatment. **B,** Flow chart showing patients and samples evaluated in the study. NA, not available; QC, quality control; UV, variants with unknown clinical significance. Created with BioRender.com.

Extraction of tumor DNA

DNA from formalin-fixed, paraffin-embedded (FFPE) tumor tissue, obtained from diagnostic cores prior to the treatment (BL), was isolated from FFPE tissue using the GeneRead DNA FFPE Kit (Qiagen) according to the manufacturer's recommendation. Briefly, the tissue sections were collected in a 1.5 mL Eppendorf tube and mixed with 1 mL xylene for 10 minutes (Sigma-Aldrich/Merck KGaA). The sections were washed three times with 100% ethanol and dried at room temperature for 10 minutes. Cells were incubated and digested with proteinase K at 56°C overnight. After heating to remove cross-links, the DNA was incubated with Uracil-N-Glycosilase (UNG) to remove deaminated cytosine residues. After washing and drying the membrane via high-speed centrifugation, DNA was eluted with 30 µL nuclease-free water (Qiagen).

Extraction of cfDNA

Cell-free DNA (cfDNA) was isolated using the QIAamp Circulating Nucleic Acid Kit (Qiagen) as described previously (32, 33). To this end, 400 µL of plasma (mixed with 600 µL PBS) were incubated with 100 µL proteinase K and 800 µL buffer ACL (containing 1 µg carrier RNA). After incubation at 60°C for 30 minutes, 1.8 mL Buffer ACB was added into the mixture and incubated on ice for 5 minutes. The mixture was then transferred into QIAamp Mini columns with a tube extender, which allowed the mixture to pass the QIAamp Mini membrane by vacuum force. After washing the membrane with Buffer ACW1, Buffer ACW2 and 96% to 100% ethanol, the QIAamp Mini column was centrifuged at 20,000 × *g* for 3 minutes. The column was then incubated at 56°C for 10 minutes to dry the membrane completely. cfDNA was eluted with 30 µL nuclease-free water (Qiagen).

Quantification

DNA concentrations were measured using the Qubit dsDNA BR Assay Kit or the Qubit dsDNA HS Assay Kit (Thermo Fisher Scientific) according to the manufacturer's instructions.

Mutation analysis of tumor samples

Targeted next-generation sequencing (NGS) of 93 frequently mutated genes in breast cancer (Supplementary Table S1) was performed using the QIAseq Human Breast Cancer Targeted Panel (Qiagen), which uses digital sequencing by incorporating unique molecular barcodes (UMI) into the starting DNA material prior to amplification, thereby overcoming the issues of PCR duplicates, false positives and library bias. Library preparation was performed according to the manufacturer's guidelines for FFPE DNA. Briefly, 20 to 40 ng of DNA were enzymatically fragmented, end repaired and A-tailed. Prior to target enrichment, adapters including a 12-base fully random UMI as well as was a sample index were ligated to each original DNA molecule. Target enrichment was performed using a single primer extension, in which each genomic target was enriched by one target-specific primer and one universal primer. The final library was purified with QIAseq Beads. After quantification using QIAseq Library Quant Assay Kit (Qiagen), libraries were sequenced on the Illumina NextSeq 550 instrument (Illumina) in a 150 bp paired end mode. On average, 6,932,822 reads (range, 1,156,790–23,751,966) were obtained per sample. Raw sequencing data were analyzed using the QIA-seq targeted DNA Panel Analysis pipeline, which processes the UMI information to distinguish true variants from artefacts based on smCounter V1 (34). After consensus read generation, we obtained an average coverage of 477X (range, 86–1,207). Variant allele frequency (VAF) of mutations was defined as the number of variant reads divided by the number of total reads. Variants that did not pass the predefined quality criteria from smCounter were dismissed. Moreover, synonymous variants and variants with VAFs lower than 10% were filtered. Furthermore, variants present with minor allele frequencies of >1% in population frequency databases (ExAC, GnomAD) were considered polymorphisms. The remaining variants were classified according to the American College of Medical Genetics and Genomics (ACMG) guidelines.

Copy number profiling of tumor samples using sWGS

WGS libraries of tissue DNA were prepared and sequenced as described previously (32, 35, 36). Briefly, shotgun libraries were prepared using the TruSeq DNA LT Sample Preparation Kit (Illumina) according to the manufacturer's instructions. 100 ng genomic DNA was fragmented to 350bp using the Covaris S220 (Covaris Ltd.). Libraries were sequenced on either an Illumina MiSeq or NextSeq 550 instrument (Illumina) in 76bp PE mode, aiming for 5 to 10 million reads per sample, representing a 0.1 to 0.2x coverage of the whole

genome. SCNA analysis and focal event calling was performed as described in refs. 32 and 35. To assess genetic instability, the percentage of the genome that was affected by copy-number gains or losses (fraction genome altered, FGA) was calculated, where a higher "fraction of genome altered" indicates increased genome instability. Tumor fractions from tissue samples were estimated with the ichorCNA algorithm, a probabilistic model for the simultaneous prediction of large-scale CNAs and estimation of tumor fraction, which is equivalent to tumor purity from bulk tumor analyses (37). Circos plot representing *G*-score were calculated by GISTIC (38).

Deep-seq

To validate variants identified with the QIA-seq panel, we performed an independent sequencing method (i.e., deep-seq) as described previously (39, 40). Briefly, target-specific primers covering mutations identified with the QIA-seq panel were designed and amplicon libraries were prepared from 5 to 10 ng tumor DNA and sequenced in 150bp PE run on a NextSeq 550 or MiSeq (Illumina). Sequencing data were analyzed using an *in-house* pipeline and visualized using Integrative Genomics Viewer (IGV; version 2.3.58).

SiMSen-seq

Pathogenic and likely pathogenic mutations identified in tumor tissue were tracked in cfDNA using SiMSen-seq (Simple, Multiplexed, PCR-based barcoding of DNA for SENsitive mutation detection using sequencing). This high-resolution sequencing approach allows a personalized assay design covering multiple mutations of the same patient (41, 42). All SiMSen-seq assays were designed and validated according to Ståhlberg and colleagues (41). Libraries were prepared using a three-cycle barcoding PCR step followed by an amplification step to add the sequencing adapters and patient specific indices and a bead purification step. Libraries were quantified on a Bioanalyzer (Agilent) High Sensitivity chip and sequenced on an Illumina NextSeq 550 instrument (Illumina) in 150bp single read mode aiming for one million reads per amplicon (actual average number of raw reads 639,626, range 32,297–4,883,340). Data analysis was performed using the Debarcer Tool Kit (41, 42). Considering only barcode families containing a minimum of three reads, an average consensus read depth of 2,069x (range 130–20,541) was obtained.

Sensitivity assessment of a 5-plex SiMSen-seq assay covering selected hotspot mutations using the Seraseq ctDNA Complete reference material (SeraCare) revealed a reliable detection of mutations down to a VAF of 0.1% (Supplementary Fig. S1). Therefore, samples were considered ctDNA positive if a VAF of ≥0.1% was observed.

Statistical analysis

Statistical analyses were performed according to the statistical analysis plan and included analyses based on the whole study population as well as subgroups stratified by treatment arm (NCT, NET) or tumor subtype (HR+/HER2−, TNBC). Our primary aim was to evaluate whether the presence or levels of ctDNA (assessed as the highest detectable VAF) at BL, MT, or EOT are correlated with tumor responses (pCR, RCB score). Moreover, we investigated whether clinicopathologic parameters at BL, including clinical tumor size [cm (2)] and stage (T ≥ 2 vs. T1), clinical nodal status (N0/1 vs. N2/3), tumor grade (G3 vs. G ≤ 2), Ki-67, TILs, or EndoPredict scores, were indicative of ctDNA release. As a secondary aim, we evaluated associations between driver alterations assessed from the tumor and clinicopathologic variables at BL as well as treatment outcome.

Descriptive statistics were used to assess clinical and genetic variables associated with baseline ctDNA levels and included frequencies and percentages or median and range [min, max], as appropriate. VAF comparisons were performed using the Mann–Whitney test. Fisher exact tests were used for associations between categorical variables. Associations between a continuous or ordinal and a categorical variable were calculated using Kruskal–Wallis tests. To assess the association between two continuous or ordinal variables, Spearman correlations were performed. Univariate and multivariate logistic regression models were used to evaluate the effects of the different covariables on response. Covariables significant in the univariate models were included in multivariate models. In cases of highly correlated variables, only one of the variables was included in the multivariate model. *P* values <0.05 were considered statistically significant. Due to small patient numbers (especially within subgroups), various analyses outlined in the statistical analysis plan were not possible and were therefore omitted.

Data availability statement

All sequencing raw data have been deposited at the European Genome-phenome Archive (EGA; http://www.ebi.ac.uk/ega/), which is hosted by the EBI, under the accession number EGAS00001005798.

Results

Patient cohort

This study included 193/400 (48.3%) patients from the prospective, randomized, multicenter phase II ABCSG-34 trial (21) with sufficient biopsy material and a tumor purity of ≥30%. Of those, 187/193 (96.8%) DNA samples passed our initial quality assessment and could be successfully sequenced with the QIAseq panel (**Fig. 1B**). The majority of patients (134/187, 71.7%) received NCT (HR+, $n = 74$; TNBC, $n = 57$; missing, $n = 3$) and 53/187 (28.3%) patients received NET as their preoperative SoC treatment (**Table 1**, left column). In the NCT arm, 41/134 (30.6%) patients achieved complete or near-complete remission (RCB 0/I), whereas patients in the NET arm had lower response rates (6/53, 11.3% achieved RCB 0/I). A pCR was observed in 27/134 (20.1%) undergoing NCT, but only in one patient (1/53, 1.9%) in the NET arm. In general, patients in the NCT arm were younger and had more aggressive disease characteristics (higher tumor grade and Ki-67, more frequently nodal-positive) compared with those treated with NET. Patient characteristics for the subset, of which plasma DNA was available ($n = 145$), were similar (**Table 1**, right column) and both cohorts were representative for the entire ABCSG-34 study population (21).

Molecular characterization of primary tumors

In 173/187 tumor samples (92.5%), at least one somatic mutation could be identified, indicating a broad patient coverage of the QIAseq breast cancer panel (**Fig. 1B**). A total of 465 somatic mutations were detected with an average of 2.6 mutations per tumor (range 1–9). As previously reported, in HR+ tumors significantly mutated genes included *PIK3CA* (32.3%), *TP53* (22.8%), and *GATA3* (16.5%; **Fig. 2A**; Supplementary Fig. S2A; refs. 43, 44). In contrast, in TNBC, *TP53* was mutated in 81.0% of tumors (**Fig. 2A**; Supplementary Fig. S2B). After variant prioritization/classification, 292 mutations (62.8%) in 156/187 tumor samples (83.4%) were classified as driver mutations (pathogenic or likely pathogenic; Supplementary Figs. S3A and S2B). Using an alternative sequencing approach (deep-seq), more than 99% of those mutations were confirmed and the VAFs were strongly correlated between QIAseq and deep-Seq

Table 1. Characteristics of patients per type of therapy.

		Patients with available tumor data			Patients with available plasma data			
Variable		***NCT*** ***n* = 134 (%)***	***NET*** ***n* = 53 (%)***	***Total*** ***n* = 187**		***NCT*** ***n* = 102 (%)**	***NET*** ***n* = 43 (%)**	***Total*** ***n* = 145**
Age	≤50	72 (53.7)	.	72	≤50	55 (53.9)	.	55
	>50	59 (44.0)	53 (100)	112	>50	44 (43.1)	43 (100)	87
	Missing	3 (2.3)	.	3	Missing	3 (3.0)	.	3
Subtype	HR+	74 (55.2)	53 (100)	127	HR+	53 (52.0)	43 (100)	96
	TNBC	57 (42.5)	.	57	TNBC	46 (45.1)	.	46
	Missing	3 (2.3)	.	3	Missing	3 (2.9)	.	3
T-stage	T1	38 (28.4)	26 (49.0)	64	T1	26 (25.4)	19 (44.2)	45
	T2	80 (59.7)	25 (47.2)	105	T2	62 (60.8)	23 (53.5)	85
	T3	13 (9.7)	2 (3.8)	15	T3	11 (10.8)	1 (2.3)	12
	T4	3 (2.2)	.	3	T4	3 (3.0)	.	3
N-stage	N0	73 (54.4)	41 (77.3)	114	N0	57 (55.9)	33 (76.8)	90
	N1	51 (38.1)	10 (18.9)	61	N1	36 (35.2)	9 (20.9)	45
	N2	1 (0.7)	.	1	N2	1 (1.0)	.	1
	N3	2 (1.5)	.	2	N3	2 (2.0)	.	2
	Missing	7 (5.2)	2 (3.8)	9	Missing	6 (5.9)	1 (2.3)	7
Grading	G1	.	8 (15.1)	8	G1		8 (18.6)	8
	G2	32 (23.9)	40 (75.5)	72	G2	23 (22.5)	30 (69.8)	53
	G3	97 (72.4)	4 (7.5)	101	G3	76 (74.5)	4 (9.3)	80
	Missing	5 (3.7)	1 (1.9)	6	Missing	3 (3.0)	1 (2.3)	4
Endopredict MS score	Low risk	NA			Low risk	4 (3.9)	20 (46.5)	24
	High risk	NA			High risk	45 (44.1)	23 (53.5)	68
	Missing	NA			Missing	53 (52.0)	.	53
EPclin	Low risk	NA			Low risk	6 (5.9)	26 (60.5)	32
	High risk	NA			High risk	41 (40.2)	17 (39.5)	58
	Missing	NA			Missing	55 (53.9)	.	55
RCB	RCB 0/I	41 (30.6)	6 (11.3)	47	RCB 0/I	33 (32.3)	5 (11.6)	38
	RCB II/III	86 (64.2)	44 (83.0)	130	RCB II/III	62 (60.8)	36 (83.7)	98
	Missing	7 (5.2)	3 (5.7)	10	Missing	7 (6.9)	2 (4.7)	9
	pCR	27 (20.1)	1 (1.9)	28	pCR	24 (23.5)	1 (2.3)	25
	No pCR	103 (76.9)	50 (94.3)	153	No pCR	74 (72.6)	41 (95.4)	115
	Missing	4 (3.0)	2 (3.8)	6	Missing	4 (3.9)	1 (2.3)	5

Abbreviation: EndoPredict MS, 12-gene Molecular Score; EPclin, combination of the 12-gene molecular score (MS) with tumor size and the number of positive nodes, which correlates to the risk of distant recurrence.

(Spearman correlation, $R = 0.9206$) (Supplementary Fig. S4). Copy number profiling was informative in 185 tumor samples and revealed significantly amplified regions, including well-known driver genes, such as 8p11.22 (*FGFR1*), 11q13.4 (*CCND1*), 12q14 (*MDM2*), or 8q24 (*MYC*; **Fig. 2A**; Supplementary Fig. S2C).

ctDNA detection in plasma during NST

Specific SiMSen-seq assays were designed for driver mutations (classified as pathogenic or likely pathogenic) identified from tissue sequencing for each patient with available plasma samples. Taken together, we screened for a total of 263 targets in 145 patients (Supplementary Table S2). In 77/145 (53.1%) and 37/145 (25.5%), one or two mutations were tracked, respectively, and in the remaining 31 patients (21.4%), between three and six targets were analyzed (**Fig. 2B**). Of those patients with more than one mutation tracked, an average of 52%, 48%, and 43% of the screened mutations could be detected at BL, MT, and EOT, respectively. Interestingly, in cases for which several mutations were screened, it was mostly the known driver mutations such as *PIK3CA* hotspot mutations that could be detected (**Fig. 2C**). For a detailed list of the mutations and their VAFs in tissue and plasma, please see Supplementary Table S2.

Prior to therapy initiation, ctDNA could be detected in 63/145 (43.4%) successfully analyzed samples (**Fig. 3A**). Of those, ctDNA persisted in 25/63 (39.7%) patients and 6/82 (7.3%) initially negatively tested patients had ctDNA detected at MT. Of those, 18/31 (58.1%) remained positive at EOT. In 28 patients, ctDNA became undetectable at MT and remained undetected at EOT in 22 of them, whereas in three patients (all RCB III) with no detectable ctDNA at MT, ctDNA reoccurred at EOT (**Fig. 3A**). Although presence of ctDNA at BL was not associated with tumor response, ctDNA detection at MT was significantly associated with higher RCB (OR 0.062; 95% CI, 0.01–0.48; $P = 0.0077$; **Fig. 3B**). Of 31 patients with detectable ctDNA at MT, 30 patients (96.8%) were nonresponders (RCB II, $n = 8$; BCB III, $n = 22$) and only one patient achieved a RCB I (**Fig. 3C**). Overall, none of the patients with RCB 0 and only 6.7% of patients with RCB I had ctDNA detected at MT, whereas 30.6% and 29.6% of patients with RCB II/III had a positive ctDNA result (**Fig. 3D**). After stratification per treatment arm, similar results were observed for patients undergoing NCT (OR = 0.064; 95% CI, 0.01–0.451; $P = 0.0095$; **Fig. 3B**). However, the association could not be confirmed in the NET study arm due to the complete or quasi-complete separation of data points. Likewise, presence of ctDNA at EOT revealed a significant association with treatment response in the entire cohort and the NCT arm, but to a lesser extent (**Fig. 3B**). When looking at pCR as response, only ctDNA at MT revealed a significant association (**Fig. 3E**). Moreover, ctDNA levels at BL were associated with treatment outcomes (median RCB0/I VAF 0.40% vs. RCBII/III VAF 0.89%; $P = 0.0449$, two-tailed Mann–Whitney test; **Fig. 4A**). Except for one patient, all patients with pCR

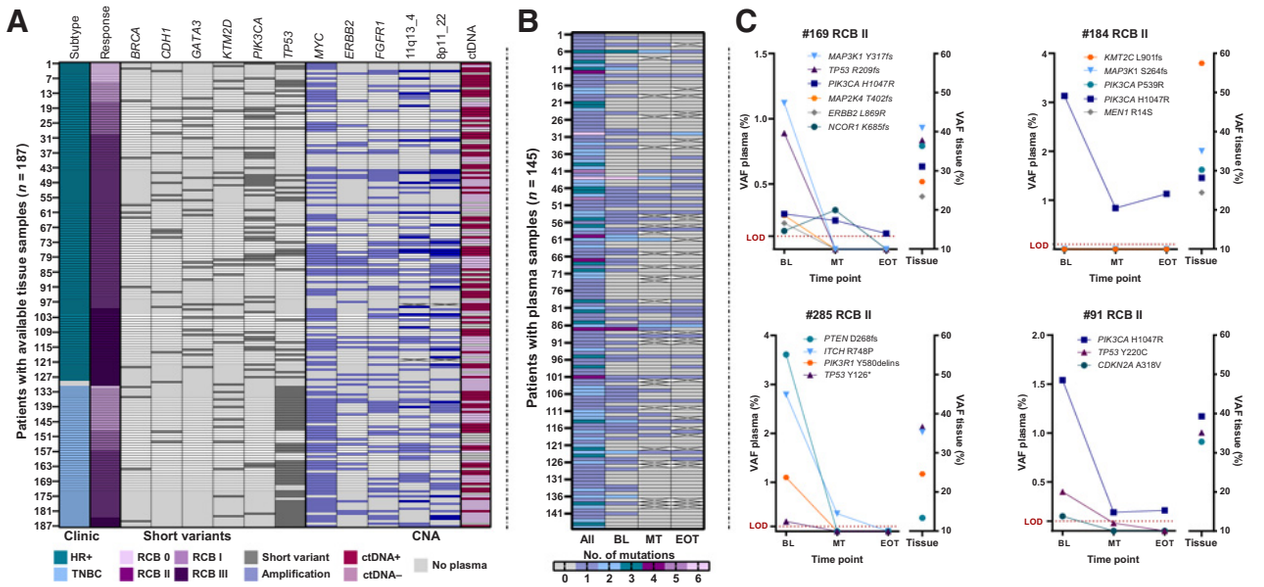

Figure 2.

Somatic driver alterations in tumor and plasma. **A,** Heat map representing the landscape of somatic driver alterations, including mutations and CNAs in tumor samples. **B,** Heat map representing number of mutations detected by SiMSen-seq in all plasma samples (All), at BL, MT, and EOT. **C,** Time courses of exemplary patients with various numbers of screened mutations in plasma. Shown are the VAF in plasma at BL, MT, and EOT (left *y*-axis) and the VAFs of the mutations detected in matched tissue samples (right *y*-axis). LOD, limit of detection.

and RCB I and detectable ctDNA at BL had decreasing levels, whereas nonresponders showed mixed ctDNA responses (**Fig. 4B** and **C**). Neither ctDNA detection rates nor levels at BL, MT, and EOT differed between HR+ and TNBC (Supplementary Fig. S5).

Association of ctDNA release at BL and clinicopathologic variables

Presence of ctDNA was significantly associated with higher stages (T1 vs. T2/3/4, Fisher exact test, $P = 0.0195$), positive lymph node status (cN+ vs. cN−, Fisher exact test, $P = 0.0200$; **Fig. 5A**), and a higher (continuous) number of intratumoral TILs (Kruskal–Wallis, $P = 0.0378$; **Fig. 5B**; Supplementary Table S3). When ctDNA was detected, patients with Ki-67 high (≥20%) tumors and higher stages had significantly higher ctDNA levels (Kruskal–Wallis test, $P = 0.0336$; Supplementary Table S4). Moreover, a weak but significant correlation was observed for the entire cohort between intratumoral TILs and BL ctDNA levels (Spearman correlation, $R = 0.2554$, $P = 0.0433$). An association with the EndoPredict clinical score revealed a borderline significance (high vs. low risk, Fisher exact test, $P = 0.0699$; Supplementary Table S3).

Association of driver events assessed from tissue with clinicopathologic characteristics

As a secondary aim, we investigated whether the presence of specific driver alterations in the tumor tissue is associated with clinicopathologic characteristics and included all patients for whom mutation ($n = 187$) and copy number ($n = 185$) data were available. Considering the entire cohort, genetic instability—reflected by the fraction of the genome affected by SCNA—and a higher number of focal amplifications was associated with higher tumor grade, higher tumor stage, higher Ki-67 scores as well as a higher number of TILs (stromal and intratumoral). For subgroup analyses and correlations with continuous values see (Supplementary Tables S5 and S6). *TP53* mutations were significantly associated with higher tumor grade, higher Ki-67 scores and TILs in the entire cohort and HR+ tumors (Supplementary Table S7). Conversely, *PIK3CA* mutations were associated with lower grading and lower Ki-67 scores (Supplementary Table S8). None of the other tested driver alterations (see **Fig. 2C**) achieved statistical significance (data not shown).

Predictive performance of driver alterations from tissue

Since recent data have indicated that valuable prognostic information can be derived from somatic driver alterations (45), we tested whether such driver events might indicate therapeutic response in our cohort. In the population as a whole, presence of high-level amplifications (HLAMP) was significantly associated with an improved response rate when measured by RCB (OR = 1.11; 95% CI, 1.02–1.20; $P = 0.0129$; Supplementary Fig. S6A). Moreover, the presence of *TP53* mutations was associated with improved response rates (OR = 2.64; 95% CI, 1.33–5.22; $P = 0.0054$). In contrast, *PIK3CA* mutations were associated with a poor tumor response (OR = 0.37; 95% CI, 0.14–0.94; $P = 0.0366$). However, in a subgroup analysis based on the tumor subtype, this association did not maintain significance. For subgroup analyses and pCR as an endpoint see (Supplementary Figs. S6B, S6C, and S7A–S7C).

Discussion

In this study, we investigated the predictive value of ctDNA for response to NST in patients with early breast cancer. To this end, we analyzed 193 patients recruited to the ABCSG-34 trial who were treated with standard NCT or NET alone or combined with tecemotide, respectively. On the basis of the molecular profile of the core biopsies assessed with a 93-gene panel, we designed personalized SiMSen-seq assays to track ctDNA during treatment. Persistence of ctDNA, particularly at mid-therapy, indicated treatment failures,

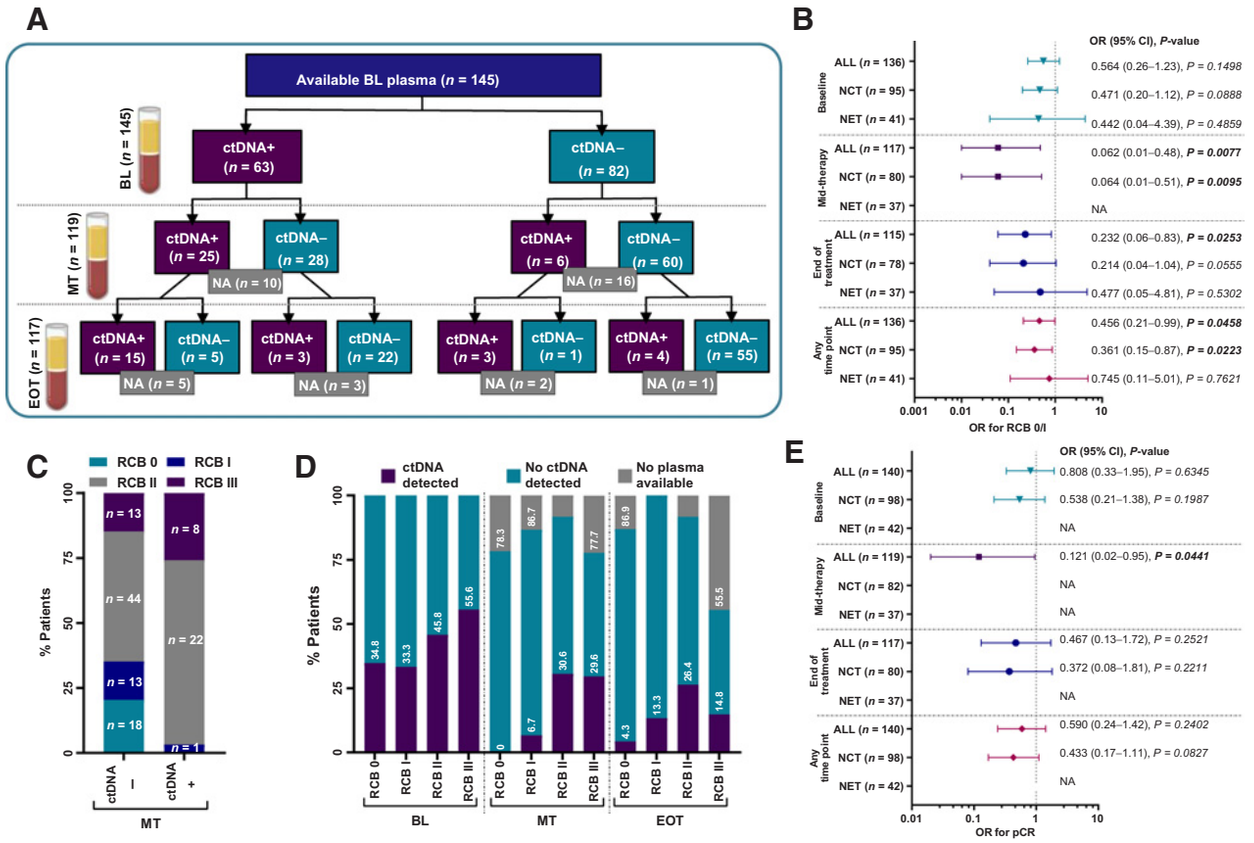

Figure 3.

Predictive value of ctDNA. **A,** Flow chart depicting patients with (ctDNA+) and without (ctDNA−) detectable ctDNA at BL, MT, and EOT. NA, no plasma available. **B,** OR with 95% confidence intervals (CI) and *P* values for ctDNA detection at BL, MT, EOT, or all time points to predict tumor response (RCB 0/I vs. RCB II/III) calculated from univariate logistic regression models. **C,** Plotted are the fractions of patients stratified by response (RCB 0–III) with (ctDNA+) and without (ctDNA−) detectable ctDNA at MT. **D,** Detection rates of ctDNA at BL, MT, and EOT stratified by RCB scores (**E**) same as in **B** but for pCR. NA, not analyzable.

whereas patients in whom ctDNA became undetectable from baseline to mid-therapy were associated with excellent responses. Overall, our results demonstrate that the detection and persistence of ctDNA at mid-therapy has the potential to negatively predict response to neoadjuvant treatment and to identify patients who will not achieve pCR or will be classified with RCB II/III. Our data confirm previous observations that dynamic monitoring of ctDNA during NST could provide an early endpoint of treatment efficacy. A noninvasive identification of RCB may in the future have the potential to aid clinical decision-making, for example with respect to treatment escalation (or de-escalation), identifying patients who might not derive benefit from breast surgery after NST, or identifying nonresponders who are known to benefit from additional adjuvant therapy. Clinical studies addressing escalation designed for patients who do not achieve pCR, like CREATE X (46) and KATHERINE (47), demonstrated a clinical benefit and with MT ctDNA, the escalation after surgery may be either predicted or intensified prior to surgery. Novel antibody–drug conjugates are now being evaluated based solely on pCR. Still, randomized, prospective studies are needed to evaluate the clinical utility of ctDNA detection during NST as evidence for treatment escalation. Furthermore, a subgroup of patients who achieve pCR after NST might not derive benefit from breast surgery after NST and the identification of those patients might minimize unnecessary invasive treatment.

An important novelty of our study is the analysis of RCB as a further endpoint of the ABCSG-34 trial in addition to pCR. Although pCR is the most commonly used pathologic staging system to risk-stratify patients following completion of neoadjuvant chemotherapy for breast cancer (48), the value of RCB as an indicator of long-term survival for patients after NST has been recognized (24, 31) and validated (49, 50). A stratification into good response classes (RCB 0/I) and bad response classes (RCBII/III) provides prognostic information for all molecular subtypes and neoadjuvant treatment regimens. Patients with RCB-I were confirmed to have similar 5-year distant relapse rates as RCB-0, whereas patients with RCB-III showed poor prognosis with a 5-year distant relapse rate of 53.6% (51). Several studies integrated RCB with other prognostic biomarkers, such as TILs (26, 52, 53) or Ki-67 (54) to provide an improved long-term prognosis. Additional integration of a molecular ctDNA response might further enable optimization of neoadjuvant therapy.

In contrast to previous reports (19, 20), at baseline neither ctDNA positivity rate nor ctDNA levels differed significantly among breast cancer subtypes (HR+ vs. TNBC). Yet, patients with a poor tumor response (RBC II/III) had significantly higher levels compared with patient with a good response. In general, ctDNA detection in patients with low tumor burden is challenging due to low fractions of ctDNA and limited numbers of available cfDNA fragments. Therefore, several

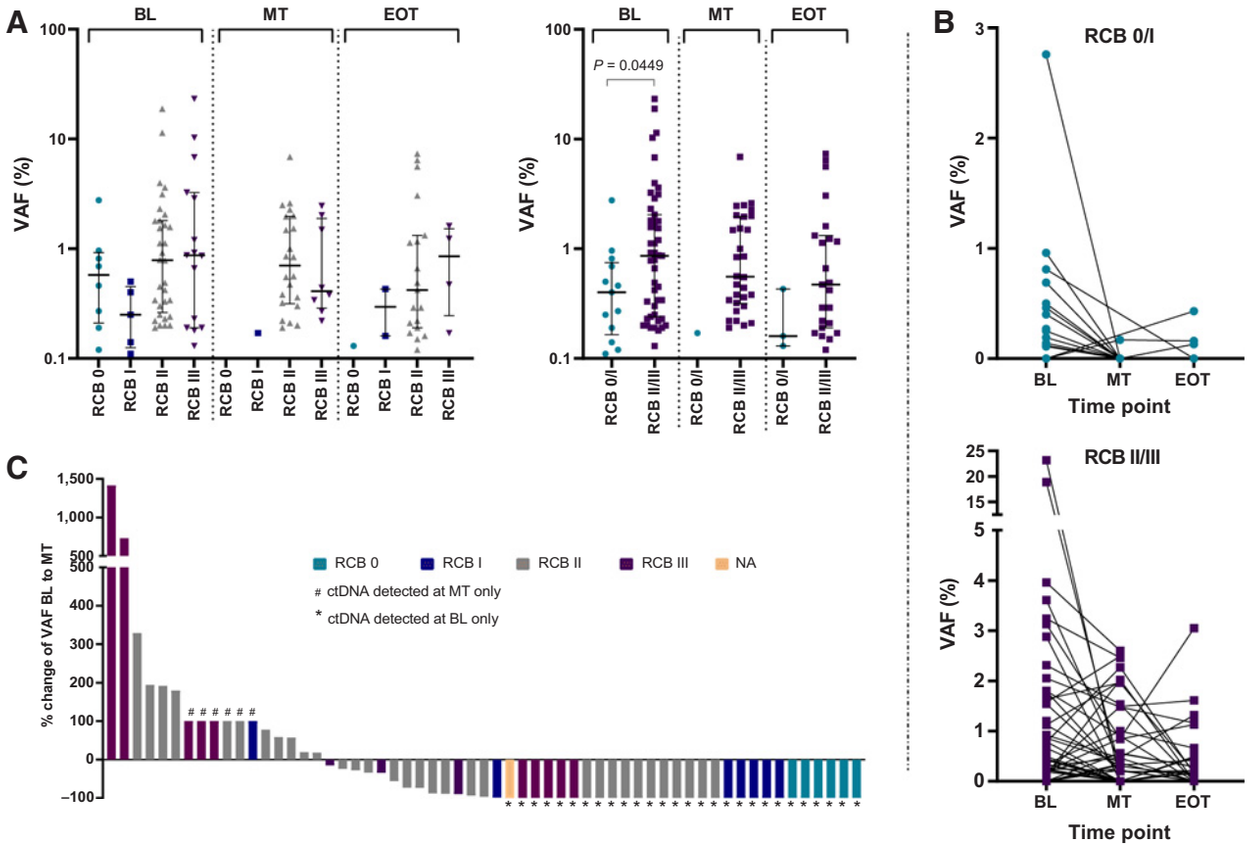

Figure 4.

ctDNA levels and dynamics over the course of neoadjuvant therapy. **A,** Plotted are VAF distributions for three time points stratified by RCB (left plot). At BL, ctDNA levels were significantly elevated in patients with poor tumor responses (RCB II/III) compared with responders (RCB 0/I). For MT and the EOT, no association could be established due to a small number of positive samples for responders (right plot). **B,** Shown are patients with ctDNA data at BL and at least one additional time point stratified by tumor response. Top plot denotes responders, lower plot represents nonresponders. **C,** Waterfall plot of ctDNA changes (in percent) from BL to MT. *, Clearance of ctDNA at MT was considered as a 100% decrease; #, ctDNA detection at MT but not at BL was considered as a 100% increase.

high-resolution technologies for detecting ctDNA have been developed in the last decade and it became clear that, in the early stages, tumor-informed approaches achieve the required sensitivity. Compared with the NeoALTO trial, in which ddPCR was performed to screen for *PIK3CA* and *TP53* mutations in 69 patients and only 41%, 20%, and 5% patients before NAT, at week 2, and before surgery, respectively, had detectable ctDNA (19), our tumor-informed analysis revealed improved detection rates. In contrast to our data, baseline ctDNA detection before NAT was associated with decreased odds of achieving pCR, but not with DFS (19). Another group employed a customized ddPCR assessment of *TP53* mutations and reported ctDNA detection in 27/36 patients (75%; ref. 17). Although in this study pCR was not correlated with ctDNA detection at any time point, ctDNA positivity after one cycle of NCT was associated with shorter DFS and OS. More recent studies have employed whole-exome sequencing (WES) of the tumor tissue to select suitable, patient-specific targets for ctDNA analyses. One such tumor-guided ctDNA analysis strategy is targeted digital sequencing (TARDIS) for multiplexed analysis of 8 to 16 patient-specific cancer mutations (55). This assay detected ctDNA in 32/32 patients with a median VAF of 0.11%. Consistent with our data, ctDNA levels were lower and showed a larger decrease in patients who achieved pCR (55). The most comprehensive study was recently published by Magbanua and colleagues, who for the first time reported an association of ctDNA with both response and survival in early breast cancer (20). The integration of genome-wide patient-specific mutational signatures may further increase the sensitivity of ctDNA analyses in early-stage patients, because a higher number of mutations tracked in plasma increases the probability of catching mutated fragments. Recently, a comprehensive analysis at a genome-wide level as an alternative to deep sequencing has been suggested (56). However, paired WGS of tumor tissue and plasma DNA including follow-up samples might still be prohibitively expensive for a ctDNA test that may have to be repeated multiple times.

Furthermore, we aimed to elucidate molecular and genomic factors predictive of ctDNA release. Presence of ctDNA was significantly associated with a higher stage and a positive lymph node status. Moreover, higher ctDNA levels were significantly associated with higher proliferation rates confirming previous reports in breast and lung cancer (20, 57). Interestingly, presence of ctDNA was also associated with intratumoral TILs, whereas stromal TILs only had borderline significance. These data may suggest that a combination of ctDNA and TILs may help identify patients who will benefit from novel neoadjuvant treatments with immune checkpoint inhibitors. Nonetheless, a subgroup analysis was not sufficiently powered.

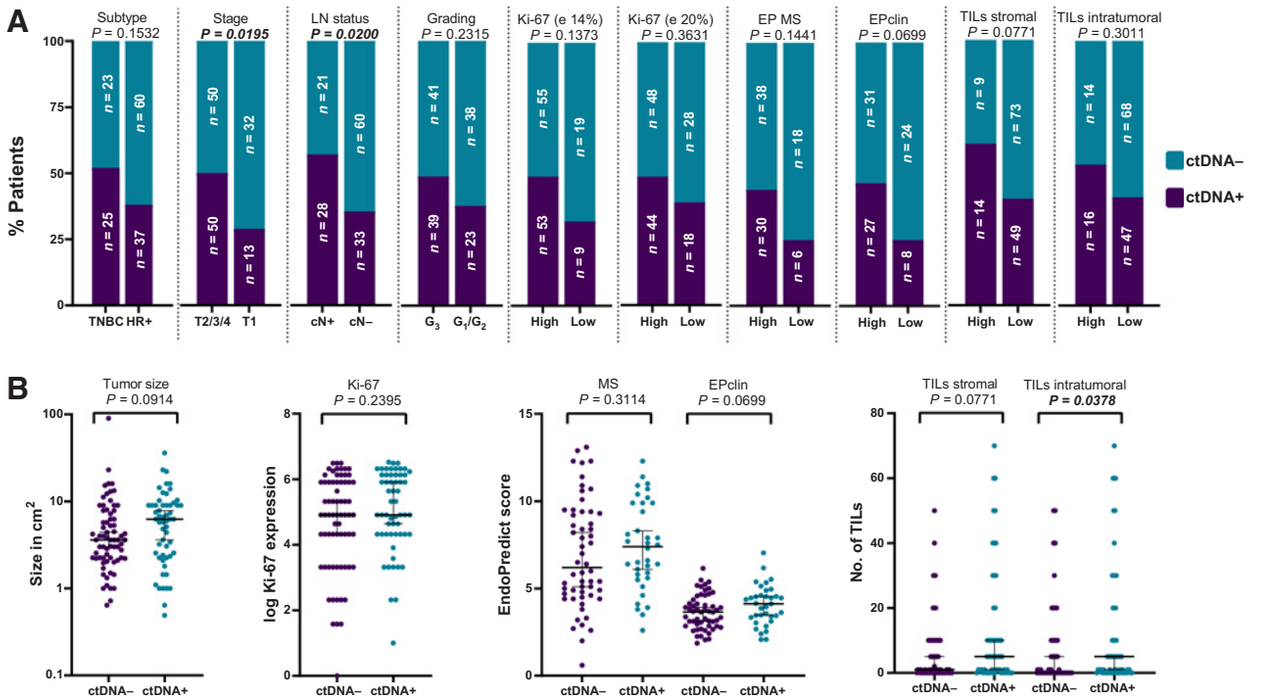

Figure 5.

Association between circulating tumor DNA and clinicopathologic characteristics. **A,** Association between ctDNA presence (ctDNA+) and absence (ctDNA−) at baseline and clinicopathologic characteristics. *P* values were calculated using Fisher exact test. **B,** Distribution of tumor size, Ki-67 scores, EndoPredict scores (MS, 12-gene molecular score; EPclin, combined clinic-molecular score), and stromal and intratumoral TILs in patients with (ctDNA+) and without (ctDNA−) detectable ctDNA at baseline.

Because EndoPredict scores were determined in a subset of ABCSG-34 patients and demonstrated that the 12-gene molecular score could predict RCB after treatment (25), we checked for associations with ctDNA detection. Although more patients with high EndoPredict clinical scores had ctDNA detected, this association did not reach statistical significance.

We also investigated the association of driver alterations with clinicopathologic factors and treatment response. As expected, the majority of TNBC tumors carried *TP53* mutations, whereas *PIK3CA* mutations were most commonly observed in the HR+ tumors. In line with a previous meta-analysis, the presence of *TP53* mutations was associated with good response in patients who received NCT (58). However, a comparison of response rates independent of the mutation status revealed that this association mainly arrived from the tumor subtype. In the NCT arm, TNBC were 2.9- and 3.5-fold more likely to achieve RCB 0/I or pCR, respectively ($P = 0.0074$), compared with HR+ tumors. Although HR+ tumors with *TP53* mutations were 2.1-fold (95% CI, 0.6–6.7) more likely to respond to NCT, this association was not significant. Nevertheless, for *PIK3CA*-mutated tumors, a chemo-free targeted approach with NET in combination with targeted treatments including CDK4/6 and PI3K inhibitors and beyond might be considered (59).

Our study has several limitations. First of all, although the ABCSG-34 clinical trial was prospective, the analyses of ctDNA were a retrospective, translational study and for definitive proof of the clinical utility of ctDNA in this setting, prospective, interventional trials are required, some of which are already underway. Moreover, because our assay detected ctDNA in only less than half of the patients, more sensitive approaches including the analysis of a large number of mutations in combination with the use of lager plasma volumes, or even multiparameter assays may have greater potential for implementation in future studies. In addition, the small number of responders in the NET impaired the statistical analyses in this subgroup. Finally, late outcomes (disease-free survival, DFS; overall survival, OS) were not available as endpoints for our study; however, pCR are RCB were repeatedly shown as strong primary endpoints. Overall, our study confirms the great promise of ctDNA as an early response marker in EBC patients undergoing NST.

Authors' Disclosures

S.P. Gampenrieder reports personal fees from Novartis, Roche, Pfizer, Lilly, AstraZeneca, MSD, Astellas, Sanofi, Seagen, Amgen, Shire, and Celgene and grants and personal fees from Daiichi Sankyo outside the submitted work. S. Frantal reports grants from Merck during the conduct of the study. G. Rinnerthaler reports personal fees from Roche, Novartis, Pfizer, Eli Lilly, Daiichi Sankyo, Gilead, MSD, and AstraZenaca outside the submitted work. C.F. Singer reports nonfinancial support and other support from Merck during the conduct of the study as well as grants, personal fees, and nonfinancial support from Novartis and AstraZeneca; grants and personal fees from Roche and Pierre Fabre; grants and nonfinancial support from Amgen and Sanofi-Aventis; and personal fees and nonfinancial support from Gilead outside the submitted work. D. Egle reports personal fees and nonfinancial support from AstraZeneca, Novartis, Pfizer, and Roche and personal fees from Amgen, Daiichi Sankyo, Lilly, MSD, and Gilead outside the submitted work. G. Pfeiler reports grants and personal fees from Pfizer, Roche, and Accord and personal fees from Novartis, Lilly, AstraZeneca, UCB, MSD, and Daiichi outside the submitted work. R. Bartsch reports personal fees from AstraZeneca, Eisai, Eli Lilly, MSD, Pierre-Fabre, Novartis, Roche, Seagen, and Puma; grants, personal fees, and nonfinancial support from Daiichi-Sankyo; and personal fees and nonfinancial support from Pfizer outside the submitted work. A. Pichler reports grants from ABCSG during the conduct of the study as well as grants from Novartis, Radius, Celgene, Roche, ABCSG, and AGMT outside the submitted work.

E. Petru reports other support from Medical University of Graz during the conduct of the study. P. Dubsky reports grants from Cepheid; grants and nonfinancial support from Roche; and other support from AstraZeneca and MSD outside the submitted work. Z. Bago-Horvath reports other support from Daichii Sankyo and personal fees from Roche outside the submitted work. C. Fesl reports grants from Merck during the conduct of the study. A. Ståhlberg reports grants from Region Västra Götaland, Sweden, Swedish Cancer Society, Swedish Research Council, the Swedish state under the agreement between the Swedish government and the county councils, the ALF-agreement, and Sweden's Innovation Agency during the conduct of the study as well as grants from Swedish Childhood Cancer Foundation and Sweden's Innovation Agency and other support from Tulebovaasta, SiMSen Diagnostics, and Iscaff Pharma outside the submitted work; in addition, A. Ståhlberg has a patent for Protection of barcodes during DNA amplification using molecular hairpins issued to Boston University and Ontario Institute for Cancer Research, a patent for Lymphocye clonality determination pending, and a patent for Compositions and methods for cell-free nucleic acid isolation pending, and reports employment with Sahlgrenska University Hospital, Gothenburg, Sweden, and University of Gothenburg, Gothenburg, Sweden. M. Filipits reports personal fees from AstraZeneca, Biorad, Boehringer Ingelheim, Eli Lilly, Merck, and Novartis outside the submitted work. M. Gnant reports personal fees from Amgen, Daiichi Sankyo, AstraZeneca, Eli Lilly, LifeBrain, Veracyte, Novartis, and Pierre Fabre outside the submitted work. M. Balic reports other support from ABCSG during the conduct of the study as well as personal fees from Amgen, AstraZeneca, Pierre Fabre, Daichii, Gilead, and Seagen; personal fees and other support from Eli Lilly, Pfizer, Roche, and MSD; grants, personal fees, and other support from Novartis; and grants and personal fees from Samsung outside the submitted work. E. Heitzer reports grants from Austrian National Bank and Austrian Federal Ministry for Digital and Economic Affairs (Christian Doppler Research Fund) during the conduct of the study as well as other support from Servier, personal fees from Roche, and grants from Freenome and PreAnalytiX outside the submitted work. No disclosures were reported by the other authors.

Authors' Contributions

Q. Zhou: Formal analysis, investigation, methodology, writing–original draft, writing–review and editing. **S.P. Gampenrieder:** Conceptualization, resources, writing–review and editing. **S. Frantal:** Data curation, formal analysis, investigation, writing–review and editing. **G. Rinnerthaler:** Conceptualization, resources, writing-review and editing. **C.F. Singer:** Resources, writing–review and editing. **D. Egle:** Resources, writing–review and editing. **G. Pfeiler:** Resources, writing–review and editing. **R. Bartsch:** Resources, writing–review and editing. **V. Wette:** Resources, writing–review and editing. **A. Pichler:** Resources, writing–review and editing. **E. Petru:** Resources, writing–review and editing. **P.C. Dubsky:** Resources, writing–review and editing. **Z. Bago-Horvath:** Resources, investigation, writing–review and editing. **C. Fesl:** Data curation, formal analysis, writing–review and editing. **M. Rudas:** Formal analysis, writing–review and editing. **A. Ståhlberg:** Methodology, writing–review and editing. **R. Graf:** Formal analysis, methodology, writing–review and editing. **S. Weber:** Formal analysis, methodology, writing–review and editing. **N. Dandachi:** Conceptualization, formal analysis, writing–review and editing. **M. Filipits:** Data curation, writing–review and editing. **M. Gnant:** Resources, data curation, writing–review and editing. **M. Balic:** Conceptualization, resources, formal analysis, writing–review and editing. **E. Heitzer:** Conceptualization, formal analysis, supervision, funding acquisition, investigation, visualization, methodology, writing–original draft, project administration, writing–review and editing.

Acknowledgments

We thank all the patients and their families who participated in the study. We would also like to thank Dr. Samantha Hasenleithner for her critical reading of the manuscript and her assistance with editing and language. This study was supported by the Austrian National Bank (##16971) and by the Austrian Federal Ministry for Digital and Economic Affairs (Christian Doppler Research Fund for Liquid Biopsies for Early Detection of Cancer (both granted to E. Heitzer). A. Ståhlberg was funded by the Region Västra Götaland, Sweden; Swedish Cancer Society (19–0306); Swedish Research Council (2017–01392); the Swedish state under the agreement between the Swedish government and the county councils, the ALF-agreement (716321), and Sweden's Innovation Agency.

The costs of publication of this article were defrayed in part by the payment of page charges. This article must therefore be hereby marked *advertisement* in accordance with 18 U.S.C. Section 1734 solely to indicate this fact.

Received September 7, 2021; revised October 27, 2021; accepted November 29, 2021; published first December 2, 2021.

References

1. Early Breast Cancer Trialists' Collaborative G. Long-term outcomes for neoadjuvant versus adjuvant chemotherapy in early breast cancer: meta-analysis of individual patient data from ten randomised trials. Lancet Oncol 2018;19:27–39.
2. Heil J, Kuerer HM, Pfob A, Rauch G, Sinn HP, Golatta M, et al. Eliminating the breast cancer surgery paradigm after neoadjuvant systemic therapy: current evidence and future challenges. Ann Oncol 2020;31:61–71.
3. Burstein HJ, Curigliano G, Loibl S, Dubsky P, Gnant M, Poortmans P, et al. Estimating the benefits of therapy for early-stage breast cancer: the St. Gallen International Consensus Guidelines for the primary therapy of early breast cancer 2019. Ann Oncol 2019;30:1541–57.
4. Cortazar P, Zhang L, Untch M, Mehta K, Costantino JP, Wolmark N, et al. Pathological complete response and long-term clinical benefit in breast cancer: the CTNeoBC pooled analysis. Lancet 2014;384:164–72.
5. Saura C, Hlauschek D, Oliveira M, Zardavas D, Jallitsch-Halper A, de la Peña L, et al. Neoadjuvant letrozole plus taselisib versus letrozole plus placebo in postmenopausal women with oestrogen receptor-positive, HER2-negative, early-stage breast cancer (LORELEI): a multicentre, randomised, double-blind, placebo-controlled, phase 2 trial. Lancet Oncol 2019;20:1226–38.
6. Marinovich ML, Houssami N, Macaskill P, von Minckwitz G, Blohmer J-U, Irwig L. Accuracy of ultrasound for predicting pathologic response during neoadjuvant therapy for breast cancer. Int J Cancer 2015;136:2730–7.
7. Gampenrieder SP, Peer A, Weismann C, Meissnitzer M, Rinnerthaler G, Webhofer J, et al. Radiologic complete response (rCR) in contrast-enhanced magnetic resonance imaging (CE-MRI) after neoadjuvant chemotherapy for early breast cancer predicts recurrence-free survival but not pathologic complete response (pCR). Breast Cancer Res 2019;21:19.
8. van Loevezijn AA, van der Noordaa MEM, van Werkhoven ED, Loo CE, Winter-Warnars GAO, Wiersma T, et al. Minimally invasive complete response assessment of the breast after neoadjuvant systemic therapy for early breast cancer (MICRA trial): Interim analysis of a multicenter observational cohort study. Ann Surg Oncol 2021;28:3243–53.
9. Tasoulis MK, Lee H-B, Yang W, Pope R, Krishnamurthy S, Kim S-Y, et al. Accuracy of post-neoadjuvant chemotherapy image-guided breast biopsy to predict residual cancer. JAMA Surg 2020;155:e204103.
10. Heil J, Pfob A, Sinn HP, Rauch G, Bach P, Thomas B, et al. Diagnosing pathologic complete response in the breast after neoadjuvant systemic treatment of breast cancer patients by minimal invasive biopsy: oral presentation at the San Antonio Breast Cancer Symposium on Friday, December 13, 2019, Program Number GS5–03. Ann Surg 2020.
11. Alix-Panabieres C, Pantel K. Liquid biopsy: from discovery to clinical application. Cancer Discov 2021;11:858–73,
12. Ignatiadis M, Sledge GW, Jeffrey SS. Liquid biopsy enters the clinic: implementation issues and future challenges. Nat Rev Clin Oncol 2021; 18:297–312.
13. Heitzer E, Ulz P, Geigl JB. Circulating tumor DNA as a liquid biopsy for cancer. Clin Chem 2015;61:112–23,
14. Heitzer E, Haque IS, Roberts CES, Speicher MR. Current and future perspectives of liquid biopsies in genomics-driven oncology. Nat Rev Genet 2019;20:71–88.
15. Garcia-Murillas I, Chopra N, Comino-Méndez I, Beaney M, Tovey H, Cutts RJ, et al. Assessment of molecular relapse detection in early-stage breast cancer. JAMA Oncol 2019;5:1473–8.
16. Butler TM, Boniface CT, Johnson-Camacho K, Tabatabaei S, Melendez D, Kelley T, et al. Circulating tumor DNA dynamics using patient-customized assays are associated with outcome in neoadjuvantly treated breast cancer. Cold Spring Harb Mol Case Stud 2019;5:a003772.
17. Riva F, Bidard F-C, Houy A, Saliou A, Madic J, Rampanou A, et al. Patient-specific circulating tumor DNA detection during neoadjuvant chemotherapy in triple-negative breast cancer. Clin Chem 2017;63:691–9.

18. Moss J, Zick A, Grinshpun A, Carmon E, Maoz M, Ochana BL, et al. Circulating breast-derived DNA allows universal detection and monitoring of localized breast cancer. Ann Oncol 2020;31:395–403.
19. Rothé F, Silva MJ, Venet D, Campbell C, Bradburry I, Rouas G, et al. Circulating tumor DNA in HER2-amplified breast cancer: a translational research substudy of the NeoALTTO phase III trial. Clin Cancer Res 2019;25:3581–8.
20. Magbanua MJM, Swigart LB, Wu H-T, Hirst GL, Yau C, Wolf DM, et al. Circulating tumor DNA in neoadjuvant-treated breast cancer reflects response and survival. Ann Oncol 2021;32:229–39.
21. Singer CF, Pfeiler G, Hubalek M, Bartsch R, Stöger H, Pichler A, et al. Efficacy and safety of the therapeutic cancer vaccine tecemotide (L-BLP25) in early breast cancer: Results from a prospective, randomised, neoadjuvant phase II study (ABCSG 34). Eur J Cancer 2020;132:43–52,
22. Bartsch R, Singer CF, Pfeiler G, Hubalek M, Stoeger H, Pichler A, et al. Conventional versus reverse sequence of neoadjuvant epirubicin/cyclophosphamide and docetaxel: sequencing results from ABCSG-34. Br J Cancer 2021;124:1795–802,
23. Yau C, van der Noordaa M, Wei J, et al. Residual cancer burden after neoadjuvant therapy and long-term survival outcomes in breast cancer: a multi-center pooled analysis. Cancer Res 2020;80.
24. Symmans WF, Wei C, Gould R, Yu X, Zhang Y, Liu M, et al. Long-term prognostic risk after neoadjuvant chemotherapy associated with residual cancer burden and breast cancer subtype. J Clin Oncol 2017;35:1049–60.
25. Dubsky PC, Singer CF, Egle D, Wette V, Petru E, Balic M, et al. The EndoPredict score predicts response to neoadjuvant chemotherapy and neoendocrine therapy in hormone receptor-positive, human epidermal growth factor receptor 2-negative breast cancer patients from the ABCSG-34 trial. Eur J Cancer 2020;134:99–106.
26. Denkert C, von Minckwitz G, Darb-Esfahani S, Lederer B, Heppner BI, Weber KE, et al. Tumour-infiltrating lymphocytes and prognosis in different subtypes of breast cancer: a pooled analysis of 3771 patients treated with neoadjuvant therapy. Lancet Oncol 2018;19:40–50.
27. Denkert C, Wienert S, Poterie A, Loibl S, Budczies J, Badve S, et al. Standardized evaluation of tumor-infiltrating lymphocytes in breast cancer: results of the ring studies of the international immuno-oncology biomarker working group. Mod Pathol 2016;29:1155–64.
28. Denkert C, Kronenwett R, Schlake W, Bohmann K, Penzel R, Weber KE, et al. Decentral gene expression analysis for ER+/Her2- breast cancer: results of a proficiency testing program for the EndoPredict assay. Virchows Arch 2012;460:251–9.
29. Kronenwett R, Bohmann K, Prinzler J, Sinn BV, Haufe F, Roth C, et al. Decentral gene expression analysis: analytical validation of the Endopredict genomic multianalyte breast cancer prognosis test. BMC Cancer 2012;12:456.
30. Filipits M, Rudas M, Jakesz R, Dubsky P, Fitzal F, Singer CF, et al. A new molecular predictor of distant recurrence in ER-positive, HER2-negative breast cancer adds independent information to conventional clinical risk factors. Clin Cancer Res 2011;17:6012–20.
31. Symmans WF, Peintinger F, Hatzis C, Rajan R, Kuerer H, Valero V, et al. Measurement of residual breast cancer burden to predict survival after neoadjuvant chemotherapy. J Clin Oncol 2007;25:4414–22.
32. Heitzer E, Ulz P, Belic J, Gutschi S, Quehenberger F, Fischereder K, et al. Tumor-associated copy number changes in the circulation of patients with prostate cancer identified through whole-genome sequencing. Genome Med 2013;5:30.
33. Suppan C, Brcic I, Tiran V, Mueller HD, Posch F, Auer M, et al. Untargeted assessment of tumor fractions in plasma for monitoring and prognostication from metastatic breast cancer patients undergoing systemic treatment. Cancers (Basel) 2019;11:1171.
34. Xu C, Ranjbar MRN, Wu Z, DiCarlo J, Wang Y. Detecting very low allele fraction variants using targeted DNA sequencing and a novel molecular barcode-aware variant caller. BMC Genomics 2017;18:5.
35. Ulz P, Belic J, Graf R, Auer M, Lafer I, Fischereder K, et al. Whole-genome plasma sequencing reveals focal amplifications as a driving force in metastatic prostate cancer. Nat Commun 2016;7:12008.
36. Zhou Q, Perakis SO, Ulz P, Mohan S, Riedl JM, Talakic E, et al. Cell-free DNA analysis reveals POLR1D-mediated resistance to bevacizumab in colorectal cancer. Genome Med 2020;12:20.
37. Adalsteinsson VA, Ha G, Freeman SS, Choudhury AD, Stover DG, Parsons HA, et al. Scalable whole-exome sequencing of cell-free DNA reveals high concordance with metastatic tumors. Nat Commun 2017;8:1324.
38. Mermel CH, Schumacher SE, Hill B, Meyerson ML, Beroukhim R, Getz G. GISTIC2.0 facilitates sensitive and confident localization of the targets of focal somatic copy-number alteration in human cancers. Genome Biol 2011;12:R41.
39. Mohan S, Heitzer E, Ulz P, Lafer I, Lax S, Auer M, et al. Changes in colorectal carcinoma genomes under anti-EGFR therapy identified by whole-genome plasma DNA sequencing. PLoS Genet 2014;10:e1004271.
40. Unseld M, Belic J, Pierer K, Zhou Q, Moser T, Bauer R, et al. A higher ctDNA fraction decreases survival in regorafenib-treated metastatic colorectal cancer patients. Results from the regorafenib's liquid biopsy translational biomarker phase II pilot study. Int J Cancer 2021;148:1452–61.
41. Ståhlberg A, Krzyzanowski PM, Egyud M, Filges S, Stein L, Godfrey TE. Simple multiplexed PCR-based barcoding of DNA for ultrasensitive mutation detection by next-generation sequencing. Nat Protoc 2017;12:664–82.
42. Ståhlberg A, Krzyzanowski PM, Jackson JB, Egyud M, Stein L, Godfrey TE. Simple, multiplexed, PCR-based barcoding of DNA enables sensitive mutation detection in liquid biopsies using sequencing. Nucleic Acids Res 2016;44:e105.
43. Cancer Genome Atlas N. Comprehensive molecular portraits of human breast tumours. Nature 2012;490:61–70.
44. Aftimos P, Oliveira M, Irrthum A, Fumagalli D, Sotiriou C, Gal-Yam EN, et al. Genomic and transcriptomic analyses of breast cancer primaries and matched metastases in AURORA, the Breast International Group (BIG) molecular screening initiative. Cancer Discov 2021;11:2796–811.
45. Luen SJ, Asher R, Lee CK, Savas P, Kammler R, Dell'Orto P, et al. Association of somatic driver alterations with prognosis in postmenopausal, hormone receptor-positive, HER2-negative early breast cancer: a secondary analysis of the BIG 1–98 randomized clinical trial. JAMA Oncol 2018;4:1335–43.
46. Masuda N, Lee S-J, Ohtani S, Im Y-H, Lee E-S, Yokota I, et al. Adjuvant capecitabine for breast cancer after preoperative chemotherapy. N Engl J Med 2017;376:2147–59.
47. von Minckwitz G, Huang C-S, Mano MS, Loibl S, Mamounas EP, Untch M, et al. Trastuzumab emtansine for residual invasive HER2-positive breast cancer. N Engl J Med 2019;380:617–28.
48. Prowell TM, Pazdur R. Pathological complete response and accelerated drug approval in early breast cancer. N Engl J Med 2012;366:2438–41,
49. Suppan C, Posch F, Mueller HD, Mischitz N, Steiner D, Klocker EV, et al. Patterns of recurrence after neoadjuvant therapy in early breast cancer, according to the residual cancer burden index and reductions in neoadjuvant treatment intensity. Cancers (Basel) 2021;13:2492.
50. Müller HD, Posch F, Suppan C, Bargfrieder U, Gumpoldsberger M, Hammer R, et al. Validation of residual cancer burden as prognostic factor for breast cancer patients after neoadjuvant therapy. Ann Surg Oncol 2019;26:4274–83.
51. Li X, Wang M, Wang M, Yu X, Guo J, Sun T, et al. Predictive and prognostic roles of pathological indicators for patients with breast cancer on neoadjuvant chemotherapy. J Breast Cancer 2019;22:497–521.
52. Asano Y, Kashiwagi S, Goto W, Takada K, Takahashi K, Hatano T, et al. Prediction of survival after neoadjuvant chemotherapy for breast cancer by evaluation of tumor-infiltrating lymphocytes and residual cancer burden. BMC Cancer 2017;17:888.
53. Luen SJ, Salgado R, Dieci MV, Vingiani A, Curigliano G, Gould RE, et al. Prognostic implications of residual disease tumor-infiltrating lymphocytes and residual cancer burden in triple-negative breast cancer patients after neoadjuvant chemotherapy. Ann Oncol 2019;30:236–42.
54. Sheri A, Smith IE, Johnston SR, A'Hern R, Nerurkar A, Jones RL, et al. Residual proliferative cancer burden to predict long-term outcome following neoadjuvant chemotherapy. Ann Oncol 2015;26:75–80,
55. McDonald BR, Contente-Cuomo T, Sammut S-J, Odenheimer-Bergman A, Ernst B, Perdigones N, et al. Personalized circulating tumor DNA analysis to detect residual disease after neoadjuvant therapy in breast cancer. Sci Transl Med 2019;11:eaax7392,
56. Zviran A, Schulman RC, Shah M, Hill STK, Deochand S, Khamnei CC, et al. Genome-wide cell-free DNA mutational integration enables ultra-sensitive cancer monitoring. Nat Med 2020;26:1114–24,
57. Abbosh C, Birkbak NJ, Wilson GA, Jamal-Hanjani M, Constantin T, Salari R, et al. Phylogenetic ctDNA analysis depicts early-stage lung cancer evolution. Nature 2017;545:446–51,
58. Chen M-B, Zhu Y-Q, Xu J-Y, Wang L-Q, Liu C-Y, Ji Z-Y, et al. Value of TP53 status for predicting response to neoadjuvant chemotherapy in breast cancer: a meta-analysis. PLoS One 2012;7:e39655,
59. Loibl S, Majewski I, Guarneri V, Nekljudova V, Holmes E, Bria E, et al. PIK3CA mutations are associated with reduced pathological complete response rates in primary HER2-positive breast cancer: pooled analysis of 967 patients from five prospective trials investigating lapatinib and trastuzumab. Ann Oncol 2019;30:1180,